Cancer Nano (2013) 4:13–20
DOI 10.1007/s12645-013-0033-8

ORIGINAL PAPER

Size-dependent cellular toxicity and uptake of commercial colloidal gold nanoparticles in DU-145 cells

Pallavi Vedantam · George Huang · T. R. Jeremy Tzeng

Received: 24 January 2013 / Accepted: 20 February 2013 / Published online: 9 March 2013

Abstract Urinary tract infection (UTI) is a predominant condition in prostate cancer patients. *Escherichia coli* ORN178 (EC-178) is the uropathogen that causes recurrent infection by binding specifically to adhesins of prostate cancer cells (DU-145 cells). Gold nanoparticles (GNPs) have been used in biodiagnosis of pathogens. In this study, we have investigated the binding time of EC-178 to DU-145 cells, the cytotoxicity and uptake of plain and mannose functionalized and 20 and 200 nm GNPs (D-mannan (Mn)-GNPs). We also investigated the protein corona of GNPs when incubated with fetal bovine serum to study the protein corona which decides the biological fate of the GNPs. It was seen that EC-178 binds and is inside the DU-145 cells by 3 h of incubation period. Plain 20 nm GNPs decrease the percentage of viable cells in 48 and 72 h in log and lag phase of DU-145 cells. It was also observed that the Mn-GNPs were taken up by the DU-145 cells significantly more than the plain GNPs. Protein corona was observed when GNPs were incubated with fetal bovine serum which was confirmed by dynamic light scattering measurements and SDS-PAGE gel.

Keywords Gold nanoparticles · *E. coli* · DU-145 cells · Mannose · Urinary tract infection · Cytotoxicity · Biodiagnostic · Protein corona · Cell uptake

1 Introduction

The estimated risk of prostate cancer is 21 % and the lifetime risk of death is 2–5 %. Even though it can be diagnosed early and therapy can be started immediately, patients developing metastatic conditions die. Apart from the potent issue of cancer, recurrent urinary tract infection (UTI) is one of the most prevalent symptoms (Klein and Thompson 2012). *Escherichia coli* ORN178 are the most common cause of UTI in humans. Various urovirulence factors of *E. coli* ORN178 have been identified such as molecular biology of surface receptors of the urothelial cells of the urinary tract, the adhesin specificity and primarily and the type 1 fimbriae associated with the organism (Sokurenko et al. 1997). Detection, diagnosis, and treatment of UTI play an important role in prostate cancer. One of the novel tools currently vastly studied are nanoparticles. Nanoparticles continue to be used as carriers for localized drug diffusion to treat and detect infections and diseases like cancer (Chen et al. 2008). Owing to their *nano* size, it is easy for these particles to diffuse into the cells and effect desired responses in treatment of diseases. However, the size, type, and surface charges of the particles play a vital role. Of the different kind of nanoparticles, gold nanoparticles (GNPs) have been extensively studied in this regard. It has been shown that *E. coli* ORN178 binds specifically to D-mannose, which is an integral part of the glycoproteins that are a part of the adhesive domain on host cells (Sharon 2006). The fimbriae of the uropathogenic *E. coli* ORN178 bind to the urolapkins on the surface of urothelial cells of the human bladder. We have demonstrated D-mannose functionalized 200 nm GNPs bind specifically to *E. coli* ORN178 (Vedantam et al. 2012). Continuing in the same direction in this study, we attempt to see if GNPs can be used as specific biodiagnostic tool to detect and treat UTI in prostate cancer cells (DU-145). This study investigates the binding time of *E. coli* ORN178 and *E. coli* ORN208 to DU-145 cells. It has been shown that *E. coli* ORN178 binds specifically to D-mannose only and *E. coli* ORN208 serves as a negative control as it has type 1 pili that fail to bind to D-mannose. In order to study the cytotoxicity of plain and functionalized 20 and 200 nm GNPs to

P. Vedantam (✉) · G. Huang · T. R. J. Tzeng
Department of Biological Sciences, Clemson University, Clemson, SC 29634, USA
e-mail: pvedant@g.clemson.edu

DU-145, growth curve of the prostate cancer cells was done. Cytotoxicity tests in log and lag phase were performed to study their biocompatibility in vitro. Cellular uptake of GNPs was estimated and protein corona of GNPs was studied (Table 1).

2 Materials and methods

The strains *E. coli* ORN178 and 208 were provided by Dr. Chu-Cheng Lin, Department of Zoology, National Taiwan Normal University and were transformed with plasmid pGREEN by electroporation (Sambrook and Russell 2001). Two different GNPs: 20 and 200 nm were purchased from Ted Pella Inc., USA. The concentration of 20 nm GNPs was 7×10^{11} particles/ml and 200 nm GNPs was 7×10^{8} particles/ml. The sugar D-mannan (Mn) was purchased from VWR (USA). The sugar was dissolved in 0.3 M sodium phosphate buffer. Surface functionalization of GNPs with the Mn was carried out by a modified multistep procedure (Aslan et al. 2004; Vedantam et al. 2012). All chemicals required for functionalizing GNPs were purchased from VWR, USA.

Human prostate carcinoma cell line DU-145 was graciously given by Dr Arun Sreekumar, Baylor College of Medicine, Houston, TX, USA. Dulbecco's modified Eagle's medium (DMEM) was modified to contain Earles Balanced Salt Solution, non-essential amino acids, 2 mM L-glutamine, 1 mM sodium pyruvate, and 1,500 mg/L sodium bicarbonate. It was supplemented with fetal bovine serum to a final concentration of 10 %, 100 UI/ml penicillin G, and 100 μg/ml streptomycin in a humidified incubator with 5 % at 37 °C. All the media components were purchased from Promega, USA.

2.1 Binding of *E. coli* to DU-145 cells

An eight-well chamber slide was used to perform the bacterial cell adhesion assay to DU-145 cells. A total of 0.5 ml of DU-145 cells (1.5×10^{6}cells/ml) was seeded in each well. The chamber slide was incubated at 37 °C overnight for attachment and fresh media was added. Fresh cultures of *E. coli* ORN178 (EC-178) and *E. coli* ORN208 (EC-208) were cultured overnight in Tryptic Soy Broth with ampicillin (50 μg/ml). The cultures were washed and resuspended in sterile PBS. A 100 μl (3×10^{8} cells/ml) aliquot of EC-178 and 208 was added to two wells each in the chamber slide. The slide was incubated for 1, 2, and 3 h. At the three different time periods, wells were washed with PBS and images were taken by a fluorescent scope (Zeiss LSM-510).

Table 1 Hydrodynamic size distribution of GNPs

Sample	Size (nm)	Zeta potential (mV)
20 nm GNP	24±2.1	−54.4
Protein coated 20 nm GNP	66.61±2.3	−18.2
200 nm GNP	213.5±2.9	−49.3
Protein coated 200 nm GNP	261.9±5.3	−13.3

2.2 DU-145 cell growth curve

Cells were plated 96-well microtiter plates at initial densities of 1,000, 2,000, 4,000, and 8,000 cells per well. The cell culture medium was changed every 3 days. Cell growth was tested by the CellTiter 96® AQueous One Solution Cell Proliferation Assay (MTS) purchased from Promega, USA. It is a colorimetric method for determining the percentage of viable cells that are proliferating. Briefly, the MTS tetrazolium is bioreduced by the viable cells into a colored formazan product which is stable and can be measured at an absorbance of 490 nm. The amount of formazan produced is directly proportional to the number of living cells in the well. MTS assays were performed every day after seeding until day 8. All the experiments were carried out in triplicates.

2.3 Cytotoxicity of GNPs to DU-145 cells

The cytotoxicity of plain GNPs was tested by CellTiter 96® AQueous One Solution Cell Proliferation Assay (MTS) purchased from Promega, USA. Cytotoxicity was measured in both the logarithmic and stationary phase of cell growth. For cytotoxicity measurements in the logarithmic phase, each cell line was incubated for 72 h in 96-well plate before adding the GNPs. Fresh medium containing increasing three different concentrations of the GNPs (10, 50, and 100 μl) was added to each well and the cells were incubated for 6, 24, 48, and 72 h time periods. The same was done for testing cytotoxicity in the stationary phase. MTS assay was performed and the percentage of cell viability was determined.

2.4 Cell uptake assay of plain and Mn-GNPs

DU-145 cells (10 ml) were seeded in a cell culture dish containing 2×10^{6} cells and cultured overnight. Once the cells were 70 % confluent, they were treated with plain and mannose functionalized 20 and 200 nm GNPs (50 μl). After 3 h of incubation, the unbound GNPs in the cell culture treatments were removed by washing the cells with PBS buffer twice. The cells were trypsinized with Trypsin–EDTA and centrifuged. After removal of the supernatant, the cells were resuspended in PBS to a final volume of 5 ml. At this stage, the total number of cells was quantified with a hemocytometer. Five milliliters of 50 % nitric acid (HNO_3) was added to each sample to lyse the cells. Inductively

coupled plasma mass spectrometry was performed to measure the gold mass in the various samples. The total number of GNPs was calculated via the gold mass. The total number of GNPs in the solution was divided by the number of cells to determine the number of GNPs taken up by the cells (Connor et al. 2005).

2.5 Cytotoxicity of functionalized GNPs to DU-145 cells and *E. coli* ORN178

The cytotoxicity of functionalized Mn-GNP of 200 nm particles was carried out by adding 200 μl of DU-145 cells (1.5×10^6 cell per well) into a 96-well plate. After incubation at 37 °C for 24 h, the cells were treated with 200 nm Mn-GNPs, 200 nm Mn-GNPs with bacteria EC-178 and 208. A total of volume 50 μl of 200 nm Mn-GNPs was added. A preincubated mix, 1 ml of the 200 nm Mn-GNPs and 1 ml of the microorganisms was incubated at 37 °C with shaking for 1 h. The solution was centrifuged and washed with sterile PBS and resuspended in sterile PBS before adding to the 96-well plates. Different plates were set up for 6-, 12-, 24-, 48-, and 72-h time periods. The MTS assay was performed and the cell viability was determined.

2.6 Protein corona of commercial 20 and 200 nm GNPs

We wanted to study the protein adsorption of the commercial 20 and 200 nm GNPs to fetal bovine serum (FBS) in DU-145 cell culture media and DMEM. The 20 and 200 nm GNPs were incubated with DMEM and cell culture medium for 1 h at 37 °C. The 20 nm GNPs samples were spinned down at 10,000×*g* for 10 min. The soups from FBS and DMEM samples were saved. The pellet containing the particles was washed thrice with nanopure water at 10,000×*g*. The particles were finally resuspended in nanopure water. The 200 nm GNPs were spinned down at 2,655×*g* for 10 min. The soups from FBS and DMEM samples were saved. The pellet containing the particles was washed thrice with nanopure water at 2,655×*g*. The particles were finally resuspended in nanopure water. Samples of pure nanoparticles of both 20 and 200 nm GNPs, DMEM and cell culture medium were also included to compare the binding of the FBS proteins to the nanoparticle surface. SDS-PAGE was performed for all the samples using a 4–20 % gel (Biorad, USA). The gel was stained by Coomassie blue stain. A Smart Protein standard (Genscript, USA) was used to identify and analyze the presence of FBS bound to the samples. The gel bands were cut up and image taken accordingly. The hydrodynamic size of the plain GNPs and protein-bound GNP samples were measured using dynamic light scattering (DLS) using Malvern Zetasizer.

2.7 Statistical analysis

All experiments were carried out in triplicates with results expressed as mean±standard error. Statistically significant differences were calculated using the two-tailed unpaired *t* test or one-way analysis of variance with *p* values of ≤0.05, <0.01, and <0.001 considered significant using Prism 5.0 (GraphPad Software, CA, USA).

3 Results

3.1 Binding of *E. coli* to DU-145 cells

The binding of EC-178 and 208 to DU-145 was studied for 1, 2, and 3 h. Phase contrast images were taken as shown in Fig. 1. It was seen that the EC-208 cells did not bind to DU-145 cells at all during all the three time periods which is expected as it serves as a negative control (Fig. 1b). On the contrary, the EC-178 cells tend to bind to the cell wall of the DU-145 cells at 2-h time period (Fig. 1d). After the 3-h time period, they appear to be inside the DU-145 cell line (Fig. 1e). Due to the wash step after time periods, it is seen that only few cells manage to bind and enter the cell line between 2 and 3 h.

3.2 DU-145 cell growth curve

In order to quantify the toxicity of the 20 and 200 nm GNPs in DU-145 cells, a growth curve was carried out. Since cells that actively grow and divide during the logarithmic growth should be more vulnerable to toxic metallic particles than cells that are nearing or at the stationary phase of cell culture. Thus, the growth curve was determined to estimate the logarithmic and stationary growth phases in relation to the number of cells seeded into each well of a 96-well culture plate (Fig. 2). It was observed that the cells reach the logarithmic phase by 3–4 days of incubation. By the eighth day, the stationary phase kicks in.

3.3 Cytotoxicity of GNPs to DU-145 cells

The cytotoxicity of 20 and 200 nm GNPs at the different time points in log phase is shown in Fig. 3. It is seen that the 20 nm GNPs seem to have a significant effect on the DU-145 cells only after 48 and 72 h of incubation period in all the three concentrations. Not much difference in viability is observed by 200 nm GNPs in the log phase when compared to 20 nm GNPs. It is seen that the size did not cause much decrease or increase in cell viability. In case of the stationary phase (Fig. 4), the cytotoxicity of 20 and 200 nm GNPs is significant as they show 24–31 % reduction in cell viability

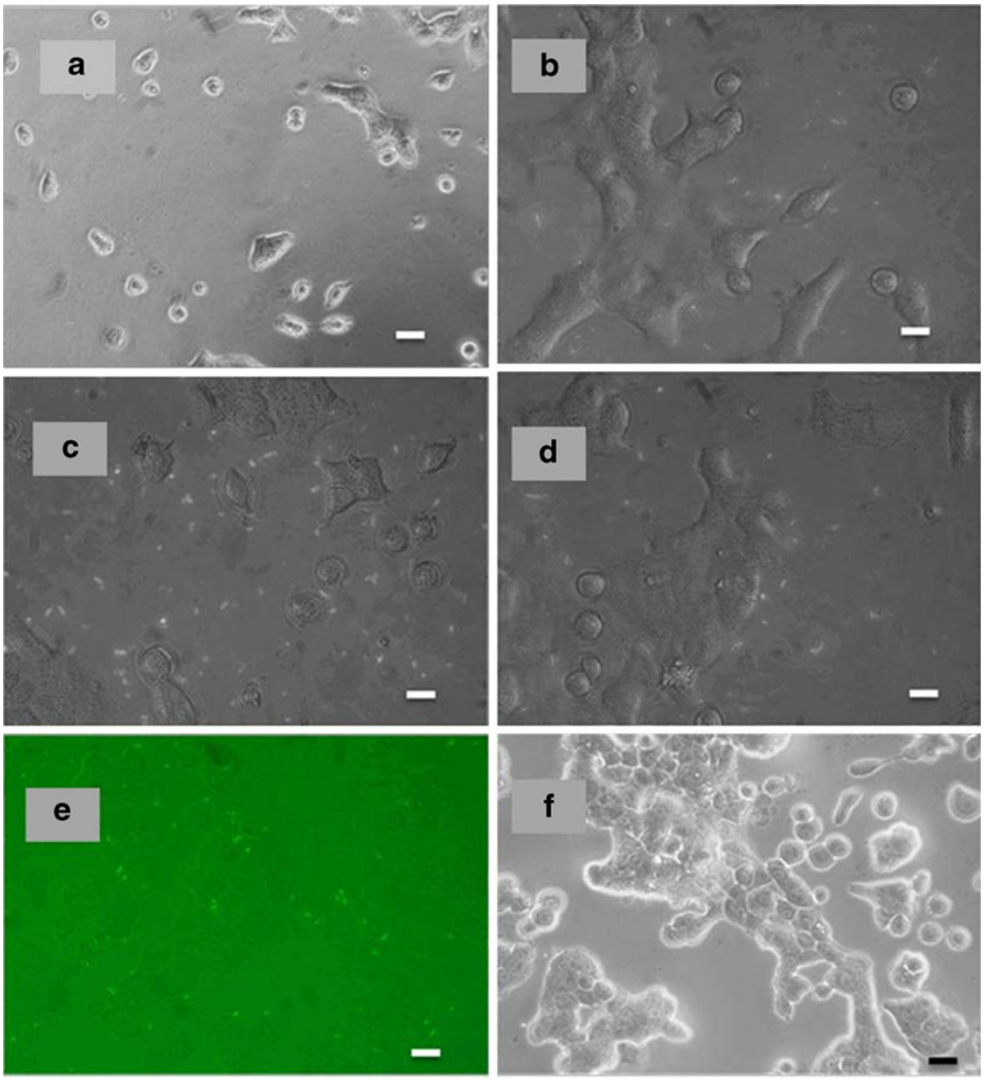

Fig. 1 **a** DU-145 cells with EC-178 at 0 min, **b** DU-145 cells with EC-208, **c** DU-145 cells with EC-178 at 1 h, **d** bright field flourescent image of DU-145 cells with EC-178 at 2 h, **e** DU-145 cells with EC-178 at 3 h, **f** control DU-145 cells. ×200 magnification. *Scale bar* 10 μm

at midrange of concentration (50 μl) compared to other low and high concentrations. Hence, it was observed that the midrange of 50 μl volume of GNPs significantly affected the percent cell viability in both log and stationary phase.

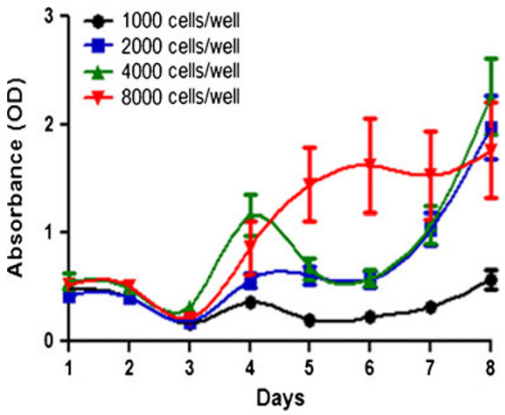

Fig. 2 Cell growth curve of DU-145 using different cell-plating numbers

3.4 Cell uptake assay of plain and Mn-GNPs

After exposure to 20 and 200 nm plain and Mn-GNPs to DU-145 cells for 3 h, the average number of GNPs per cell associated with each DU-145 cell was estimated as shown in Fig. 5. The number of GNPs per cell in DU-145 cells was 3.4×10^4 for plain 20 nm GNP where as it was 1.7×10^4 for 200 nm plain GNPs. In contrast, exposure to 20 nm Mn-GNPs results in as much twice the increase of nanoparticle uptake compared to the plain 20 nm plain GNPs. There was a significant increase in the uptake of the 200 nm Mn-GNPs, more than double the number of GNPs when compared to the plain 200 nm GNPs. There does not seem to be a significant difference between uptake levels of Mn-GNPs (both 20 and 200 nm).

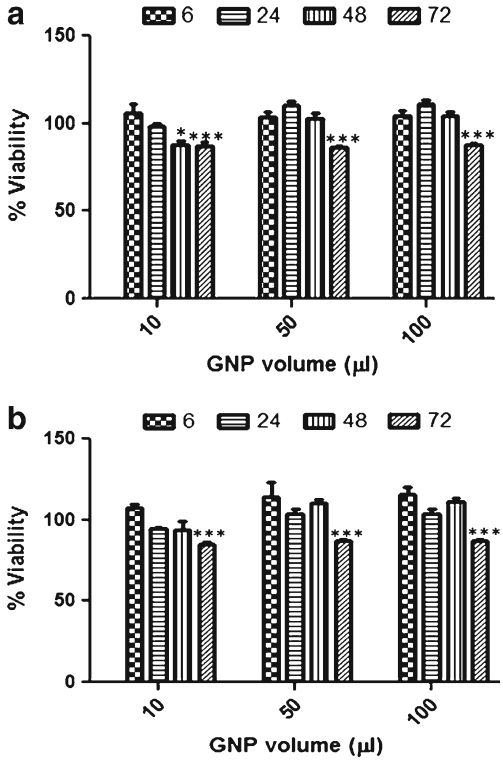

Fig. 3 Cell cytotoxicity profiles of DU-145 cells in log phase. **a** Cell viability of DU-145 in log phase when treated with plain 20 nm GNPs and **b** cell viability of DU-145 in log phase when treated with 200 nm GNPs. *$p<0.05$, ***$p<0.001$

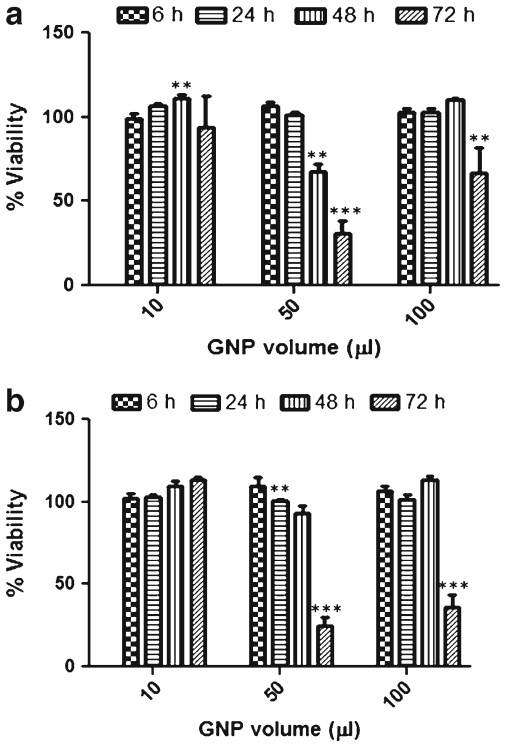

Fig. 4 Cell cytotoxicity profiles of DU-145 cells in lag phase. **a** Cell viability of DU-145 in lag phase when treated with plain 20 nm GNPs and **b** cell viability of DU-145 in lag phase when treated with 200 nm GNPs. **$p<0.01$, ***$p<0.001$

3.5 Cytotoxicity and competitive binding of functionalized GNPs to DU-145 cells and EC-178

Figure 6 shows the cytotoxicity of functionalized GNPs to the DU-145 cells at 1–6 h time points. A midrange concentration of 200 nm Mn-GNPs (50 µl) was used in this assay. After various binding assays, it was seen that 50 µl is the minimum concentration 200 nm Mn-GNPs required to effect binding. It is seen that mannose functionalized 200 nm GNPs when bound to EC-178 relatively show the same percent viability when compared to the control DU-145 cells. On the other hand, the EC-178 bacterial cells bring about cell death in about 6 h. When the 200 nm Mn-GNPs and EC178 are added together at once to the DU-145 cells, 64 % viability of the cell line is observed. But, when the 200 nm Mn-GNPs are premixed with EC-178 and then added to the DU-145 cell 73 % viability is observed. This shows that when they are premixed the functionalized GNPs bind to EC-178 and prevent the binding of the latter to DU-145, thereby increasing the cell viability. Even though the increase is not significant, it shows that there could be competitive binding between EC-178 and 200 nm Mn-GNPs to bind to DU-145 cells. This also suggests that the Mn-GNPs could competitively bind to the cell surface that has mannose residues and there by block the attachment of bacteria to those mannose residues on the DU-145 cell surface receptors (Miura et al. 2001).

3.6 Protein corona of GNPs

The hydrodynamic sizes of the plain and protein coated GNPs did increase when incubated with FBS (Fig. 7). The DLS measurements indicate that the protein in FBS did adsorb and hence the increase in diameter. The 20 nm GNPs were found to be of 66.61±2.3 nm size and the 200 nm showed increase in size were of 261.9±5.3 nm. This

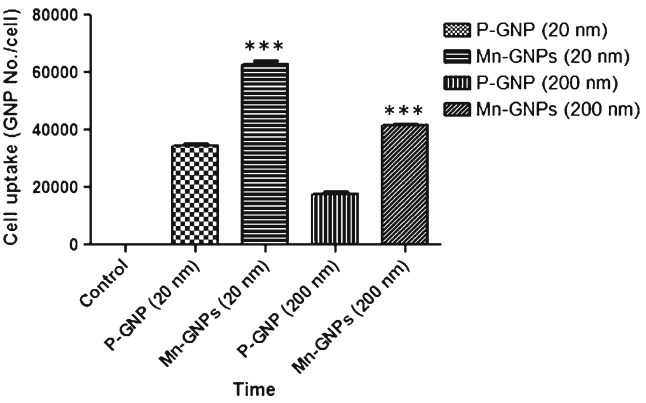

Fig. 5 DU-145 cell uptake of plain GNPs (P-GNP) and mannose functionalized GNPs (Mn-GNPs). ***$p<0.001$

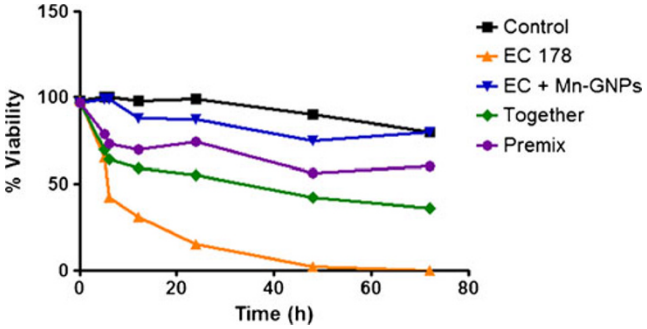

Fig. 6 DU-145 cell growth pattern with different treatments at 6-, 12-, 24-, 48-, and 72-h time points

confirms the presence of protein corona which remained coated even after multiple washes. The zeta values do show good stable protein coated 20 and 200 nm GNPs (Table 1). The SDS-PAGE gel was done to confirm the same (Fig. 8). The 20 and 200 nm GNPs (arrow marks) do confirm the presence of protein corona with a clear thick band. The samples incubated with plain DMEM did not show any bands at all. Hence, it is clear that there was protein bound to the GNPs.

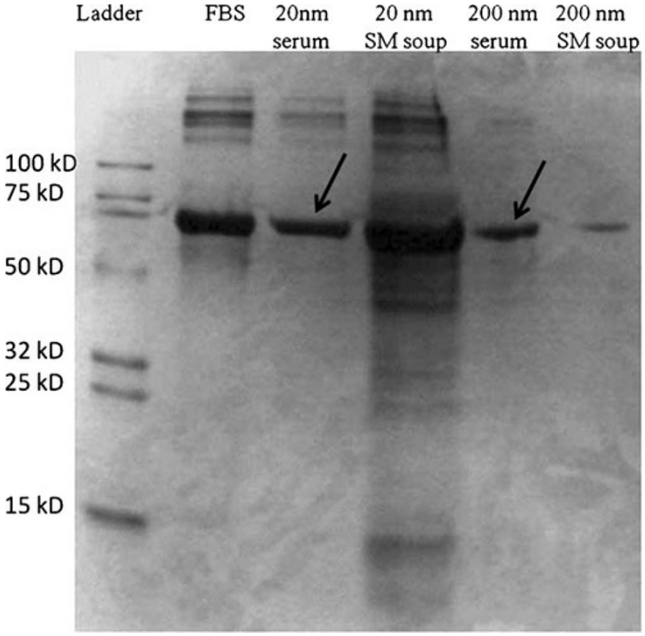

Fig. 8 Coomassie-stained SDS-PAGE gel lanes for protein coated 20 and 200 nm GNPs. FBS is a combination of various proteins. The lanes "20 nm serum and 200 nm serum" show a band for protein bound to the GNPs suggesting the presence of protein corona. The samples incubated with plain DMEM did not show any protein bands (data not shown)

4 Discussion

Application of chemotherapy with GNPs is a new treatment approach in cancer therapy (Lehmann et al. 2008). There has been extensive research done and many underlying reasons have been identified for the invasiveness of prostate cancer. Cell–cell adhesion molecules that are involved in cell aggregation are calcium-dependent moieties known as cadherins. When there is a dysfunction in the cadherin pathway cancer tumor tends to become invasive. E-cadherin is a marker of carcinogenesis in prostate cancer. The cadherin family proteins have mannose residues on their cell surface receptors (Paul et al. 1997). These mannose residues also are detected by the uropathogenic bacteria *E. coli*. Keeping this in mind, the 200 nm GNPs were only functionalized with mannose to test adhesion and cytotoxicity. The bigger size GNPs were used to functionalize with mannose than 20 nm GNPs because due to their increased size. If they bind to the DU-145 cells and competitively block the mannose residues from becoming available for uropathogenic bacteria. Also, if the Mn-GNPs do bind to the prostate cancer cells, then the uropathogenic bacteria can detect, and chemotactically and specifically adhere to the mannose bound to GNPs. Once, many bacteria are bound to the GNPs, due to their bigger size and the peristaltic flow near the tissue, the GNP-bacterial complex could be dislodged and can be detached from the prostate cancer cells. If this happens, then the severity of the UTI can also be diagnosed, treated, and prevented. As it was seen that the DU-145 cells are actively reproducing in log phase by 48 h of incubation, the cytotoxicity profiles indicated that there is no significant toxicity at all in 6- and 24-h incubated periods. Hence, Mn-GNPs can be safely used for detection or treatment of prostate cancer or UTI. The viability profiles of DU-145 cells also indicate that the plain and Mn-GNPs do significantly decrease the viable cells by 48–72 h of incubation. Hence, if Mn-GNPs are used as a drug carrier can bring about

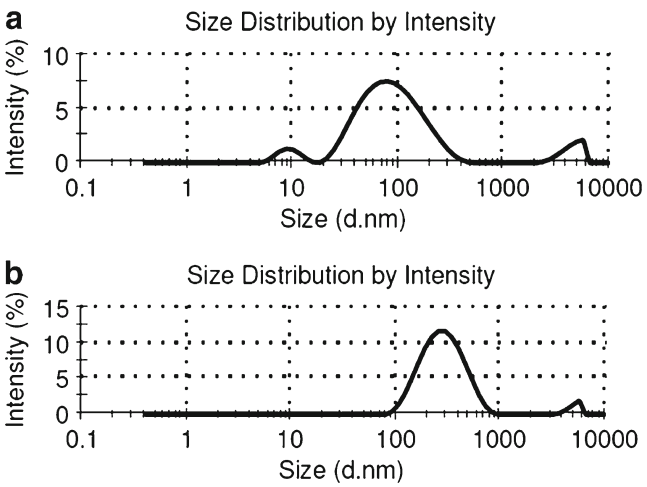

Fig. 7 Hydrodynamic size distribution of **a** protein-coated 20 nm GNP and **b** protein-coated 200 nm GNP

synergistic killing of the prostate cancer and such a treatment is could be localized treatment and site directed when introduced locally.

Compared to the 20 nm plain and Mn-GNPs were taken up by the DU-145 cells, more than the 200 nm plain and Mn-GNPs. It has been documented that 15 nm glucose functionalized GNPs have been taken up more than the plain or chemically functionalized GNPs (Zhang et al. 2008). They have also demonstrated there is enhanced radiation sensitivity in prostate cancer by GNPs. Hence, if GNPs are functionalized with mannose sugar, they can be used as a vehicle to treat UTI. Gold nanoparticles are heavy metals with increased *f* factor that enhance radiosensitivity have been studied in mice (Hainfeld et al. 2004; Wilson et al. 2009). They attributed the sensitivity to the high-Z radio-enhancement by GNPs. Since the uptake studies of GNPs in this study indicate that 20 nm Mn-GNPs are taken up more than 200 nm Mn-GNPs, they could be used for killing the DU-145 cells in promising clinical applications if used as drug carrier. The 200 nm Mn-GNPs can be used for antiadhesion of uropathogenic bacteria in prostate cancer cells. This approach can be used for future treatment of UTI cases as there is an increase in antibiotic resistance of microorganisms.

For this, the uptake of the GNPs and their interaction with cellular proteins is essential. Hence, the protein adsorption of FBS on the 20 and 200 nm GNPs was studied. The DLS measurements and the SDS-PAGE gel indicate a strong band confirming the presence of the protein corona around the GNPs. It is crucial to know how the nanoparticles behave in blood plasma and in vivo in general. Hence, there have been many studies where the GNPs have been studied in depth to understand the protein–nanoparticle complexes in vitro to make the nanoparticles more robust and practical for various clinical applications. The chemical functionalization, size of the nanoparticle, type of proteins, and surface charges do decide the biological fate of the nanoparticle when administered for therapeutic purposes (Pan et al. 2007; Nativo et al. 2008; Arnida et al. 2010). This protein corona is important as it decides the particle's longevity in the blood stream which is very important for therapeutic efficacy. It has been shown that 30 and 50 nm citrate-stabilized gold colloids were bound to 69 different proteins in plasma (Dobrovolskaia et al. 2009). It has been also demonstrated that the kinetic and equilibrium binding properties depend on protein identity as well as particle surface characteristics and size (Cedervall et al. 2007). In order to understand the transport pathways utilized by nanoparticles, it is necessary to know how long they lived in the living system, which will determine its biological fate (Lundqvist et al. 2011). Researches have demonstrated that 15 nm GNPs form proteins/NP complexes in RPMI are more abundantly internalized in cells as compared to DMEM, overall exerting higher cytotoxic effects in HeLa cells (Maiorano et al. 2010). It is important to understand what happens to the fate of the nanoparticles once they have been utilized for biological applications.

5 Conclusion

It has been shown previously in our previous investigation that GNPs when functionalized with D-mannose bind specifically to only EC-178 (Vedantam et al. 2012). Based on this fact, our investigation attempted to carry out cytotoxicity assays with plain and Mn-GNPs it is seen that 20 and 200 nm GNPs bring out significant decrease in cell viability by 48–72 h only both in log as well as lag phase of DU-145 cells. Also, it has been shown that there might be a competitive binding between Mn-functionalized and GNPs when present together with DU-145 cells. The plain 20 nm GNPs were more inside the cell when compared to the plain 200 nm GNPs. The Mn-GNPs of 20 nm size were also taken up more compared to the 200 nm Mn-GNPs. It was also demonstrated that both 20 and 200 nm GNPs do bind to protein and form a stable protein corona. Since it has been shown that GNPs of different sizes between 20 and 100 nm have shown to alter signalling pathways in cells and mediate biological processes (Jiang et al. 2008), based on which they can be used for targeted drug delivery as well as for detection purposes. Lastly, the binding of EC-178 shows that competitive binding to Mn-GNP can be done to avoid binding of the bacteria to the DU-145 cells and hence, this mechanism can be further developed to prevent/detect recurrent UTI in prostate cancer cells.

Acknowledgments We are grateful to Dr Thompson Mefford, Department of Material Sciences, Clemson University for the use of Malvern Zetasizer. We would also like to acknowledge Dr. Sai Sathish (Sri Sathya Sai Institute of Higher Learning) and Dr Ramakrishna Podila (Research Associate in the Department of Physics and Astronomy, Clemson University) for their valuable technical assistance.

References

Arnida, Malugin A et al (2010) Cellular uptake and toxicity of gold nanoparticles in prostate cancer cells: a comparative study of rods and spheres. J Appl Toxicol 30(3):212–217

Aslan K, Lakowicz JR et al (2004) Tunable plasmonic glucose sensing based on the dissociation of Con A-aggregated dextran-coated gold colloids. Anal Chim Acta 517(1–2):139–144

Cedervall T, Lynch I et al (2007) Understanding the nanoparticle–protein corona using methods to quantify exchange rates and affinities of proteins for nanoparticles. Proc Natl Acad Sci 104 (7):2050–2055

Chen PC, Mwakwari SC et al (2008) Gold nanoparticles: from nanomedicine to nanosensing. Nanotech Sci Appl 1:45–66

Connor EE, Mwamuka J et al (2005) Gold nanoparticles are taken up by human cells but do not cause acute cytotoxicity. Small 1 (3):325–327

Dobrovolskaia MA, Patri AK et al (2009) Interaction of colloidal gold nanoparticles with human blood: effects on particle size and analysis of plasma protein binding profiles. Nanomed Nanotechnol Biol Med 5(2):106–117

Hainfeld JF, Slatkin DN et al (2004) The use of gold nanoparticles to enhance radiotherapy in mice. Phys Med Biol 49(18):N309

Jiang W, KimBetty YS et al (2008) Nanoparticle-mediated cellular response is size-dependent. Nat Nano 3(3):145–150

Klein EA, Thompson IM (2012) Chemoprevention of prostate cancer: an updated view. World J Urol 30(2):189–194

Lehmann J, Natarajan A et al (2008) Short communication: nanoparticle thermotherapy and external beam radiation therapy for human prostate cancer cells. Cancer Biother Radiopharm 23(2):265–271

Lundqvist M, Stigler J et al (2011) The evolution of the protein corona around nanoparticles: a test study. ACS Nano 5(9):7503–7509

Maiorano G, Sabella S et al (2010) Effects of cell culture media on the dynamic formation of protein—nanoparticle complexes and influence on the cellular response. ACS Nano 4(12):7481–7491

Miura H, Nishimura K et al (2001) Effects of hepatocyte growth factor on E-cadherin-mediated cell–cell adhesion in DU145 prostate cancer cells. Urology 58(6):1064–1069

Nativo P, Prior IA et al (2008) Uptake and intracellular fate of surface-modified gold nanoparticles. ACS Nano 2(8):1639–1644

Pan Y, Neuss S et al (2007) Size-dependent cytotoxicity of gold nanoparticles. Small 3(11):1941–1949

Paul R, Ewing CM et al (1997) The cadherin cell–cell adhesion pathway in prostate cancer progression. Br J Urol 1:37–43

Sambrook J, Russell D (2001) Molecular cloning: a laboratory manual. Cold Spring Harbor Laboratory Press, New York

Sharon N (2006) Carbohydrates as future anti-adhesion drugs for infectious diseases. Biochim Biophys Acta Gen Subj 1760 (4):527–537

Sokurenko EV, Chesnokova V et al (1997) Diversity of the *Escherichia coli* type 1 fimbrial lectin. Differential binding to mannosides and uroepithelial cells. J Biol Chem 272(28):17880–17886

Vedantam P, Tzeng T-R et al (2012) Binding of *Escherichia coli* to functionalized gold nanoparticles. Plasmonics 7(2):301–308

Wilson R, Xiaojing Z et al (2009) Gold nanoparticle sensitize radiotherapy of prostate cancer cells by regulation of the cell cycle. Nanotechnology 20(37):375101

Zhang X, Xing JZ et al (2008) Enhanced radiation sensitivity in prostate cancer by gold-nanoparticles. Clin Invest Med 31(3): E160–E167